RESEARCH ARTICLE

Understanding the role of nano-TiO$_2$ on the toxicity of Pb on *C. dubia* through modeling—Is it additive or synergistic?

Xuesong Liu[1,4], Jianmin Wang (✉)[1,2], Yue-Wern Huang[2,3]

1 Department of Civil, Architectural and Environmental Engineering, Missouri University of Science and Technology, Rolla, MO 65409, USA
2 The Center for Research in Energy and Environment (CREE), Missouri University of Science and Technology, Rolla, MO 65409, USA
3 Department of Biological Sciences, Missouri University of Science and Technology, Rolla, MO 65409, USA
4 State Key Laboratory of Environmental Criteria and Risk Assessment, Chinese Research Academy of Environmental Sciences, Beijing 100012, China

H I G H L I G H T S

- A two-compartment model is able to quantify the effect of nano-TiO$_2$ on Pb toxicity.
- Nano-TiO$_2$ reduces Pb tolerance level and increased the killing rate for *C. dubia*.
- Thus, nano-TiO$_2$ synergistically enhances Pb toxicity.
- Algae reduce Pb transfer rate to the body tissue and the killing rate.

G R A P H I C   A B S T R A C T
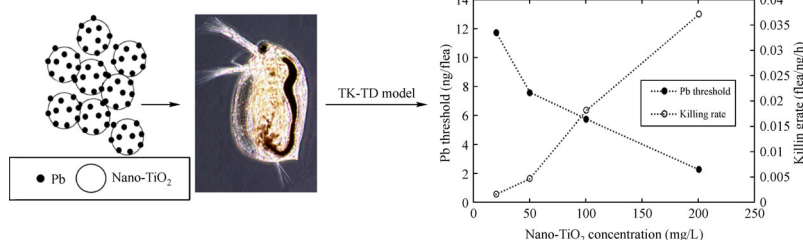
A B S T R A C T

Nano-TiO$_2$ can remarkably increase lead (Pb) toxicity in aquatic organisms. However, the mechanism of this toxicity, additive or synergistic, is not well understood. To explore this mechanism, we inspected the role of nano-TiO$_2$ in the toxicity of Pb on *Ceriodaphnia dubia* (*C. dubia*), a model water flea species typically used for ecotoxicity studies. The effect of algae, a diet for aquatic organisms, on the effect of this binary mixture was also investigated. A two-compartment toxicokinetic (TK)-toxicodynamic (TD) modeling approach was used to quantify the Pb toxicity under these complex conditions and to develop critical parameters for understanding the mechanism of toxicity. This two-compartment modeling approach adequately described the Pb accumulation in the gut and in the rest of the body tissue under different nano-TiO$_2$ concentrations, with and without algae, and predicted the toxicity response of *C. dubia*. It indicated that increasing the nano-TiO$_2$ concentration reduced the Pb tolerance level and concurrently increased the killing rate constant of *C. dubia*. Therefore, nano-TiO$_2$ synergistically enhanced Pb toxicity. Algae remarkably reduced the toxicity of this binary mixture through reducing the Pb transfer rate to the body tissue and the killing rate, although it did not affect the Pb tolerance level. This two-compartment modeling approach is useful in understanding the role of nanoparticles when assessing the overall toxicity of nanoparticles and other toxic elements in the environment.

✉ Corresponding author
E-mail: wangjia@mst.edu

1   Introduction

The release of nanoparticles (NPs) has received close attention due to their potential environmental and health risks (López-Serrano et al., 2014; Bundschuh et al., 2018). Because nano-TiO$_2$ has a low toxicity (Allen et al., 2008), it is widely used in commercial and industrial products (O'Regan and Grätzel, 1991; Lademann et al., 1999; Dudefoi et al., 2017). However, previous research has demonstrated that nano-TiO$_2$ can carry and transport

background toxins (including toxic metals) to organisms to impose toxicity, which has been commonly described as the "Trojan Horse Effect" (Fan et al., 2011; Wang et al., 2011a; Hu et al., 2012a). Because both NPs and toxic metals can produce reactive oxidation species (ROS) in organisms (Ercal et al., 2001; Li et al. 2015), this toxicity might be characterized as an additive toxicity, which is simply expressed as $1 + 1 = 2$ (Roell et al., 2017). However, toxic metals adsorbed on a nano-TiO_2 surface could form surface complexes (Vohra and Davis, 1997), which may also play an important role in toxicity (Sparks, 2005), adding another dimension to the toxicity mechanism. Therefore, in addition to the toxic effect from each individual component, nano-TiO_2 may also contribute to the toxicity in a synergistic manner, which could be characterized as $1 + 1 > 2$ (Roell et al., 2017).

A process-based toxicokinetic (TK) - toxicodynamic (TD) modeling approach has been increasingly used to assess the toxic effect of single or multiple toxins (Tan et al., 2012; Cedergreen et al., 2017). The assumption of this approach is that hazard, as indicated by the probability of death, starts to develop if the toxic element accumulation in the body exceeds a threshold concentration, or the level an organism can tolerate. The TK model quantifies toxic element accumulation in an organism, and the TD model links this accumulation with toxicity. In the TD model, two parameters, threshold concentration and killing rate, are used to define the lethality of a toxic element, and changes in these parameters reflect changes in toxicity (Tan et al., 2012).

Because toxic metals accumulated in some body parts of an organism can be readily depurated, the distribution of toxic metals within an organism is critical in its toxicity response (Gillis et al., 2005; Tan and Wang, 2012; Cai et al., 2020). Previous research also found that NPs could aggravate, which impacts metal toxicity through different pathways (Fan et al., 2011; Wang et al., 2011a; 2011b; Tan et al., 2017). Therefore, NPs can change the distribution of toxic metals in an organism and impact the toxicity. Thus, when investigating the binary toxicity of NPs and toxic metals, the conventional total accumulation approach is no longer applicable. Recently, we validated a two-compartment modeling method, including a two-compartment based TK model and a body tissue accumulation-based TD model, to quantify Pb toxicity in the presence of 50 mg/L of nano-TiO_2 on *C. dubia* (Liu et al., 2021). This modeling approach first determines Pb distribution between the gut and other body parts (e.g., the tissue) within the *C. dubia* body, and uses the Pb accumulated in the tissue to quantify the Pb toxicity. The distribution of Pb between the gut and the tissue was validated using a different method (Liu et al., 2021). Through modeling, we can determine key parameters, namely, the threshold concentration and the killing rate, to quantify the toxicity of Pb. In the present study, we applied this two-compartment modeling approach, for the first time, to develop a mechanistic understanding of the

effect of nano-TiO_2 on Pb toxicity by using parameters developed through modeling experimental data. This mechanistic understanding is essential for the assessment of the environmental impact of NPs. In addition, because algae are a common food source for aquatic creatures and could significantly reduce Pb toxicity in the presence of nano-TiO_2 (Liu et al., 2019), we also used this two-compartment modeling approach to develop an understating of the role of algae in this combined toxicity. Thus, the objectives of this research were to establish a fundamental understanding of the role of nano-TiO_2 in the toxicity of Pb, and to learn how algae impact this toxicity.

2 Materials and methods

2.1 Chemicals, NPs, and organisms

A moderate hardness culture medium buffer (hardness = 85 ± 5 mg/L as $CaCO_3$, pH = 7.8 ± 0.2) was prepared by using $NaHCO_3$ (Pb < 5 mg/kg, 100.2%), $CaSO_4 \cdot 2H_2O$ (98%), Na_2SeO_4 (99%), KCl (99%), and $MgSO_4$ (Pb < 0.001%), following EPA toxicity test protocol (EPA, 2002). $Pb(NO_3)_2$ was dissolved into Milli-Q water (18.2 M$\Omega \cdot$cm) to prepare a Pb stock solution (1000 mg/L). To prevent precipitation, the Pb stock solution was initially acidified to a pH of less than 4. All samples were acidified and digested by using trace metal grade nitric acid before Pb analysis. The calibration curves for Pb analysis were developed by diluting a certified Pb standard solution (1000 mg/L) with Milli-Q water. All of these chemicals were ACS grade and were acquired from Fisher Scientific (USA).

The 5–10 nm size nano-TiO_2 (anatase, 99%) was obtained from Skyspring Nanomaterials Inc. (USA). Dry nano-TiO_2 particles were added to 100 mL of culture medium in a 125 mL HDPE bottle to prepare a nano-TiO_2 stock solution (200 mg/L). The bottle was sealed and mixed for 10 min in a mechanical shaker. The nano-TiO_2 stock solution was freshly prepared for each test.

C. dubia was selected as the model organism for this research. The *C. dubia* was acquired from MBL Aquaculture (USA). The stock solutions of food for *C. dubia* were obtained from ABS Inc. (USA). They are green algae (*Raphidocelis*) at a concentration of 3×10^7 cells/mL, and YTC (yeasts, trout chow, and cereal leaves) at a concentration of 1700 mg/L as total solids, respectively. Appropriate volumes of these stock food solutions were spiked into a culture medium buffer for a mass culture, to achieve final concentrations of algae and YTC of 1.8×10^5 cells/mL and 6.8 mg/L as total solids, respectively. The same algae were also used in other experiments in this study. A SVC-6AX laminar flow hood, which was purchased from Streamline® laboratory products (USA), was installed in a thermostatic cabinet (25°C), and used to

conduct a mass culture and all other tests. The light: dark cycle of the temperature-controlled chamber was fixed at 16 h light / 8 h dark, to mimic the natural condition.

2.2 Accumulation test

Accumulation tests were conducted to determine the total Pb accumulation in *C. dubia* under various conditions (nano-TiO$_2$ concentration, accumulation time, and the absence/presence of algae). The experimental data were used for Pb accumulation modeling. The accumulation process was facilitated by using high dose of Pb and nano-TiO$_2$ in accordance with EPA (1994). Test solutions of 100 mL were added in 125 mL HDPE bottles for each experiment. The accumulation test includes eight test solutions. For each test solution, a total of nine reactors, representing nine exposure times, 1, 2, 4, 6, 8, 12, 16, 20, and 24 h, were used. All test solutions contained 2500 µg/L of Pb. The first five test solutions also contained nano-TiO$_2$ at concentrations of 10, 20, 50, 100, and 200 mg/L, respectively. The rest of the test solutions contained three different concentrations of nano-TiO$_2$ (50, 100, and 200 mg/L, respectively), with the same 1.8×10^5 cells/mL of algae. A control group of *C. dubia* (without contacting any of the test solution) was used to evaluate the Pb background in *C. dubia*. The pH of each test solution was 7.8±0.2. This time-dependent experimental data was used to determine the accumulation kinetic constants through modeling, and to predict Pb distribution in *C. dubia* under various experimental conditions.

For each reactor used in the accumulation test, approximately 30 adult *C. dubia* (1 week old) were first picked from the mass culture, and then washed three times with a fresh culture medium buffer before transferring to reactors. After being exposed for a pre-selected amount of time, *C. dubia* were collected from the reactor, and then washed with a fresh culture medium three times to detach particles from their surface. These collected and washed

C. dubia were then screened (0.297 mm sieve), recorded, and added to a digestion container. The organisms were digested with 5 mL nitric acid for 12 h at 95°C using a hot-block digester. The digestion temperature was controlled by a 0R10-000G Watlow mini controller (Watlow, USA). Milli-Q water was used to dilute the digested sample before conducting the analysis. The Pb accumulation in *C. dubia* under different conditions was calculated from the soluble Pb concentration in each digested sample. The Pb background in *C. dubia* was 0.10 ng/flea, which was determined from a control group. The accumulated amount of Pb in *C. dubia* was determined by deducting the background from the total accumulation. For each accumulation test, duplicate reactors were used.

A two-compartment TK model (developed in our previous publication) was used to quantify the Pb accumulation and distribution in *C. dubia* in the presence of NPs (Liu et al., 2021). In brief, in a NP-toxic metal system, toxic metals are either adsorbed by NPs, or are present in a soluble form. As an adsorbent, nano-TiO$_2$ particles adsorb nearly 100% of Pb from water (Liu et al., 2019). Next, *C. dubia* actively uptake particles, even the settled ones, through the mouth (Horton et al., 1979). *C. dubia* were characterized as the gut and other body parts (expressed as "tissue" hereafter). The Pb accumulated in the gut was impacted by three pathways: active mouth uptake, depuration from gut, and transfer from gut to tissue. The Pb accumulated in the tissue was determined by transfer from the gut and diffusion in and out of the tissue through the body surface. Because Pb diffusion in and out of the tissue through the body surface was negligible, the tissue accumulation of Pb was mainly contributed from the gut (Liu et al., 2021). The equations below (Eqs. (1)–(3)) express the kinetics of Pb gut accumulation and tissue accumulation in the presence of NPs, and the definition of symbols are shown in Table 1 (Liu et al., 2021).

$$C_T(t) = C_{gut}(t) + C_{tissue}(t), \tag{1}$$

Table 1 Toxicokinetic and toxicodynamic model symbol and parameters

Model	Symbol	Definition	Unit
Toxicokinetic	$C_T(t)$	Total Pb in the whole body at time t	ng/flea
	$C_{gut}(t)$	Pb in the gut at time t	ng/flea
	$C_{tissue}(t)$	Pb in the tissue at time t	ng/flea
	C_{Pb}	Total Pb concentration in the solution	ng/L
	C_{NP}	Total NP concentration in the solution	mg/L
	k	Active mouth uptake constant	mg/flea/h
	k_{12}	The gut to body tissue transfer constant	h^{-1}
	k_{1e}	The gut depuration constant	h^{-1}
	t	Exposure time	h
Toxicodynamic	S(t)	Survival probability of test organisms at time t	N.A.
	k_k	Killing rate	flea/ng/h
	C_{TH}	Toxic metal threshold concentration	ng/flea

$$C_{\text{gut}}(t) = \frac{\dfrac{C_{\text{pb}}}{C_{\text{NP}}} \times k}{k_{12} + k_{1\text{e}}} \times \left(1 - e^{-(k_{12}+k_{1\text{e}})t}\right), \qquad (2)$$

$$C_{\text{tissue}}\ (t)$$

$$= \frac{\dfrac{C_{\text{Pb}}}{C_{\text{NP}}} \times k \times k_{12} e^{-(k_{12}+k_{1\text{e}})t}\left(e^{(k_{12}+k_{1\text{e}})t} \times (k_{12}t + k_{1\text{e}}t - 1) + 1\right)}{(k_{12} + k_{1\text{e}})^2}.$$

$$(3)$$

2.3   Toxicity test

Eight series of 100 mL test solutions, which included five Pb concentrations (500, 1000, 1500, 2000, and 2500 μg/L) in each series, were prepared by adding the Pb stock solution, nano-TiO$_2$ stock solution, and an algae stock solution (if needed) at specific ratios into the culture medium buffer in 125 mL HDPE bottles. The ratio of clean culture medium, Pb stock solution, nano-TiO$_2$ stock solution, and algae stock solution were determined based on their concentrations that were selected for each toxicity test. The test solutions that had a Pb concentration of 2500 μg/L were prepared in duplicate. In addition to Pb, the first through fifth series of bottles also contained 10, 20, 50, 100, and 200 mg/L of nano-TiO$_2$, respectively. The sixth through eighth series of bottles also contained 50, 100, and 200 mg/L of nano-TiO$_2$, respectively, and the same 1.8 × 10^5 cells/mL of algae. This concentration of algae can support normal living of *C. dubia* (EPA, 2002). A mechanical shaker was used to mix all test solutions for 24 h. The final pH of the solutions was 7.8±0.2.

The EPA method was followed in conducting the toxicity tests (EPA, 2002). Initially, a time-dependent toxicity test was conducted using eight test solutions that had a Pb concentration of 2500 μg/L and different concentrations of nano-TiO$_2$, with and without algae. For each test solution, four parallel 30 mL reactors, with each reactor containing 15 mL of test solution, were utilized. Twenty healthy *C. dubia* neonates, aged less than 24 h, were washed with a clean culture medium buffer, and used for each test solution, with five neonates for each reactor. The neonates were transferred to the reactor by using a wide opening plastic dropper (tip diameter: 3 mm). The duration of the toxicity test was 24 h, and the survivorship of the neonates was recorded hourly. The dead neonates were removed from the reactor as soon as they were observed during the hourly checkup. To mimic the natural condition, the nano-TiO$_2$ in the reactor was not dispersed further during the test period. The time-dependent survivorship data from one set of the test solution that had 2500 μg/L of Pb were fitted with the TD model to determine relevant parameters. The rest of the solutions that had different concentrations of Pb, nano-TiO$_2$, and

algae (total eight series, with five Pb concentrations in each series) were used to conduct independent 24-h toxicity tests, to develop data for model validation. The test procedures were the same as above, except that the survivorship was checked only at the 24th h.

Equation (4) is the TD model used to quantify Pb toxicity, based on tissue accumulation, and the definition of symbols are shown in Table 1 (Liu et al., 2021).

$$S(t) = \begin{cases} 1 & \text{if } C_{\text{tissue}}(t) \leqslant C_{\text{TH}} \\ e^{-k_{\text{k}} \times \left(C_{\text{tissue}}(t) - C_{\text{TH}}\right)t} & \text{if } C_{\text{tissue}}(t) > C_{\text{TH}} \end{cases} . \qquad (4)$$

2.4   Analytical method

Soluble Pb concentrations in digested samples from the accumulation tests were determined by an AAanalyst 600 graphite furnace atomic absorption spectrometer (GFAA) (Perkin-Elmer, USA). The Pb detection limit was 0.5 μg/L.

3   Results and discussion

3.1   Nano-TiO$_2$ impact on Pb accumulation

Based on the EPA standard procedure, *C. dubia* neonates (age < 24 h) were used for the toxicity test. In theory, the same organism should have been used in the accumulation test. However, because of the fragile nature, these *C. dubia* neonates can not survive through the manual procedure that has to be followed for the accumulation test. Instead, we used adult *C. dubia* as a surrogate to conduct the accumulation test (Wang et al., 2011b; Liu et al., 2019; 2021; Liu and Wang, 2020). In this work, we acquired time-dependent accumulation data from the 24-h accumulation period using adult *C. dubia*, and used the TK model, Eqs. (1), (2), and (3), to fit these data. The filled circles in Fig. 1(a) were Pb accumulation data in the presence of 100 mg/L nano-TiO$_2$ and 2500 μg/L Pb. Accumulation data under other nano-TiO$_2$ concentrations (10, 20, 50, and 200 mg/L) are shown in Figs. S1–S4 (supplementary information). The curve fitting results for the whole body Pb accumulation are represented with a solid curve in all of these figures. The model fitting was in good agreement (all $R^2 > 0.88$) with the experimental data. Table 2 lists the accumulation kinetic parameters under all experimental conditions. The dashed curve and dotted curve were the calculated Pb accumulation in the gut and in the tissue, respectively. To validate the calculated Pb distribution within the body (in the gut and in tissue), we also conducted independent depuration tests, following a different method in our previous work, and used the depuration data to determine Pb distribution right after the accumulation period (Liu et al., 2021). They showed a good agreement with the calculated results from the
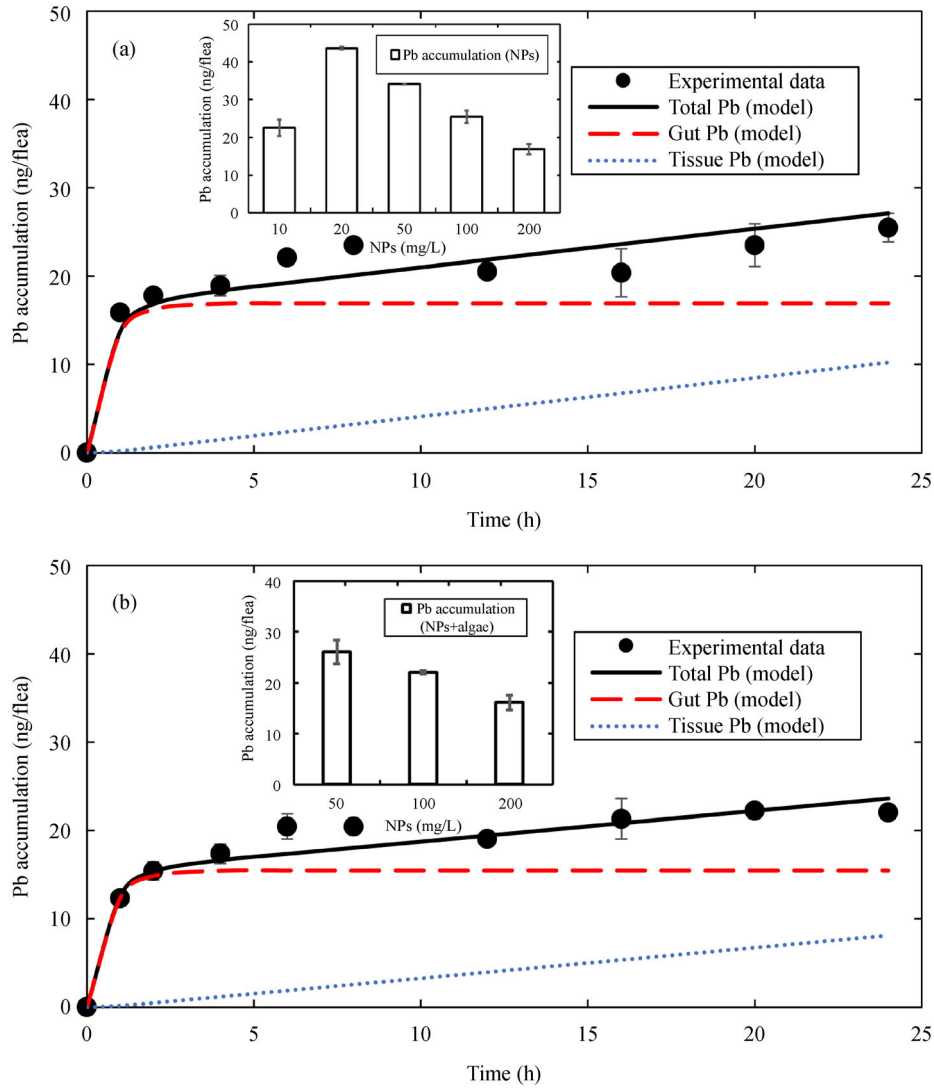
Fig. 1 The Pb accumulation in *C. dubia* in the presence of nano-TiO$_2$, with and without algae: (a) nano-TiO$_2$ + Pb, and (b) nano-TiO$_2$ + Pb + algae. Exposure medium: [Pb] = 2500 µg/L; NPs = 100 mg/L; algae = 1.8 × 10^5 cells/mL. Each filled circle point represents the average value of data (N = 2), error bars represent the range of the data. The inset is the 24-h Pb accumulation in *C. dubia* under different nano-TiO$_2$ concentrations with and without algae: (a) nano-TiO$_2$ + Pb, NPs = 10–200 mg/L, and (b) nano-TiO$_2$ + Pb + algae, NPs = 50–200 mg/L. Condition of the exposure medium: [Pb] = 2500 µg/L; algae = 1.8 × 10^5 cells/mL.

Table 2 Toxicokinetic model parameters (the gut uptake constant k, Pb transfer constant from gut to body tissue k_{12}, Pb depuration constant from gut k_{1e}) determined at the Pb concentration of 2500 µg/L

NPs (mg/L)	Algae (cells/mL)	k ($\times 10^{-3}$ mg/flea/h)	k_{12} (h^{-1})	k_{1e} (h^{-1})	R^2
10	0	0.097	0.026	1.588	0.95
20		0.395			0.88
50		0.694			0.96
100		1.091			0.91
200		1.418			0.93
50	1.8 × 10^5	0.610	0.022	1.588	0.89
100		0.998			0.95
200		1.342			0.93

accumulation model (data not shown). The modeling results showed that Pb gut accumulation reached the maximum value in approximately 2 h. However, Pb accumulation in the tissue increased slowly at a nearly constant rate. As a digestive tract, the gut could regulate nutrient transport to body tissue through active and passive mechanisms (Kiela and Ghishan, 2016). Although Pb does not serve as a nutrient for *C. dubia*, it may use nutrient channels (e.g., the calcium ion (Ca^{2+}) channel) to transfer to the body tissue continuously (Kerper and Hinkle, 1997). Consequently, the tissue's Pb content gradually increased with time. Results showed that Pb accumulated in the gut at a much faster rate as compared to that in the tissue at the beginning of the test. This was because Pb gut accumulation was mostly from active ingestion, which is a very fast process. However, Pb lacked a specific uptake pathway from the gut to the tissue, due to the non-physiologic function of Pb in cells (ICMM, 2007). Although the Ca^{2+} channel is one of the pathways for Pb transfer (Kerper and Hinkle, 1997), the test medium (moderate hardness water) had a high concentration of Ca^{2+}, which likely outcompeted Pb for its transfer to the tissue.

As indicated in Table 2, the gut uptake constant (k) was increased with nano-TiO_2 concentration. However, the Pb transfer to the tissue (k_{12}) and depuration from the gut (k_{1e}) were not changed with nano-TiO_2 concentrations. The transporters and ion channels limited the Pb transfer to the tissue (Kiela and Ghishan, 2016). Obviously, changing the nano-TiO_2 concentration would not change the number of transporters/ion channels and alter the Pb transfer rate. Within the gut, because the pH was 6.0–6.8, which was lower than the pH of the culture medium of 7.8 (Ebert, 2005), some adsorbed Pb would easily release from the nano-TiO_2 surface and depurate from the gut. Also, because pH is a dominate factor for the release of Pb from nano-TiO_2 (Hu and Shipley, 2012), changing of the nano-TiO_2 concentration would not alter the gut depuration of Pb.

Nano-TiO_2 serves as a Pb carrier (Hu et al., 2012a). Therefore, the nano-TiO_2 concentration significantly affects Pb accumulation. The inset in Fig. 1(a) shows the 24 h Pb accumulation results in the whole body under various concentrations of nano-TiO_2 without algae. It shows that the 24-h accumulation of Pb first increased with the increase in nano-TiO_2 concentration. However, when the nano-TiO_2 concentration exceeded 20 mg/L, the Pb accumulation decreased with increasing nano-TiO_2. Previously, we found that NP accumulation in *C. dubia* would increase with NP concentration until it reaches 20 mg/L, and further increase in NP concentration would not change the NP accumulation (Hu et al., 2012b). This was because *C. dubia* have a limited capacity for holding NPs (Wang et al., 2011b). In this research, nano-TiO_2 serves as a carrier of Pb. At low nano-TiO_2 concentrations ($\leqslant$20 mg/L), an increase in nano-TiO_2 increased nano-TiO_2 accumulation,

which resulted in an increase in Pb accumulation in *C. dubia*. However, when the nano-TiO_2 concentration was further increased to above 20 mg/L, the nano-TiO_2 accumulation in *C. dubia* was not increased. Rather, increasing the nano-TiO_2 concentration reduced Pb adsorption density on nano-TiO_2, thereby resulting in a decrease in the total Pb accumulation in *C. dubia*. This can be characterized as a dilution effect from nano-TiO_2.

3.2 Algae impact on Pb accumulation

Figure 1(b) shows algae impact on Pb accumulation – both the gut and the tissue Pb accumulations were reduced. However, under both conditions, the Pb exhibited the same accumulation patterns. Algae could serve as a Pb carrier (Roy et al., 1993), but its adsorption capacity was much lower than nano-TiO_2 (Liu et al., 2019). Therefore, nano-TiO_2 carried in most of the Pb that accumulated in *C. dubia*. On the other hand, algae could fill gut space and reduce nano-TiO_2 accumulation. The kinetic model suggested that the maximum Pb content in the gut was 16.9 ng without algae, but it had been slightly reduced to 15.5 ng in the presence of 1.8×10^5 cells/mL algae. Furthermore, modeling results indicated that algae (1.8×10^5 cells/mL) significantly reduced Pb tissue accumulation from 10.2 ng to 8.1 ng, which is an approximate 21% reduction.

Figures S5 and S6 (supplementary information) show the Pb accumulation data and modeling results at nano-TiO_2 concentrations of 50 and 200 mg/L, respectively, in the presence of algae. The kinetic constants for accumulation in the presence of algae are also shown in Table 2. Results suggested that algae reduced the Pb uptake constant k for all nano-TiO_2 concentrations, which agree with the above assessment. Table 2 also shows that the Pb transfer to the tissue (k_{12}) was reduced in the presence of algae. This was because algae could reduce the retention of nano-TiO_2 in the gut (Tan and Wang, 2017), thereby reducing the Pb retention time and resulting in less Pb assimilation in the tissue. However, in a real environmental condition, other factors (e.g., natural organic matter and chelates) may form organic complexes with Pb, and further compromise the reduction of Pb transfer to the tissue. Wani et al. (2015) found that organic Pb could easily pass through the cell membrane, thereby resulting in high Pb accumulation in organisms. Therefore, the presence of soluble organic matter needs to be considered when dealing with real environmental conditions.

Interestingly, Table 2 shows that algae did not change the gut depuration constant. As discussed earlier, the Pb gut depuration rate is mostly controlled by the gut pH, and the presence of algae would not change the gut pH of *C. dubia*. Therefore, the same gut depuration rate was observed. The small inset in Fig. 1(b) shows that, under the testing concentration range, Pb accumulation was reduced

with an increase in nano-TiO$_2$ concentration, which was consistent with the result from the tests without algae.

3.3 Effect of nano-TiO$_2$ on Pb toxicity – experiment data and model prediction

Figure 2(a) shows the time-dependent survivorship of *C. dubia* exposed to 2500 μg/L of Pb with various concentrations of nano-TiO$_2$ during a 24-h testing period. It shows that the survivorship decreased when nano-TiO$_2$ concentration increased. From the inset in Fig. 1(a), we noticed that the 24-h total Pb accumulation in *C. dubia* first increased with the increase in nano-TiO$_2$ concentration. However, when the nano-TiO$_2$ concentration exceeded 20 mg/L, the Pb accumulation was reduced due to a dilution effect – the higher nano-TiO$_2$ concentration

reduced the adsorption density of Pb on NPs, resulting in less Pb assimilation (Wang et al., 2011b). As indicated by the dotted lines in Figs. 1(a) and S1–S4, the model calculated Pb tissue accumulation (using parameters in Table 2 and Eq. (3)) was also reduced by increasing the nano-TiO$_2$ concentration. Apparently, the decreasing trend of the survivorship (e.g., increasing toxicity) with the increase in the nano-TiO$_2$ conflicted with the decreasing trend of the total or tissue accumulation of Pb. Nano-TiO$_2$ must have imposed an additional toxic effect. Based on experimental observation, for *C. dubia* exposed to 2500 μg/L of Pb with low nano-TiO$_2$ concentrations (10–20 mg/L), the decreased survivorship was mainly caused by the increasing Pb tissue accumulation. However, when a higher nano-TiO$_2$ concentration (50–200 mg/L) was applied, the Pb content in the tissue decreased, but the
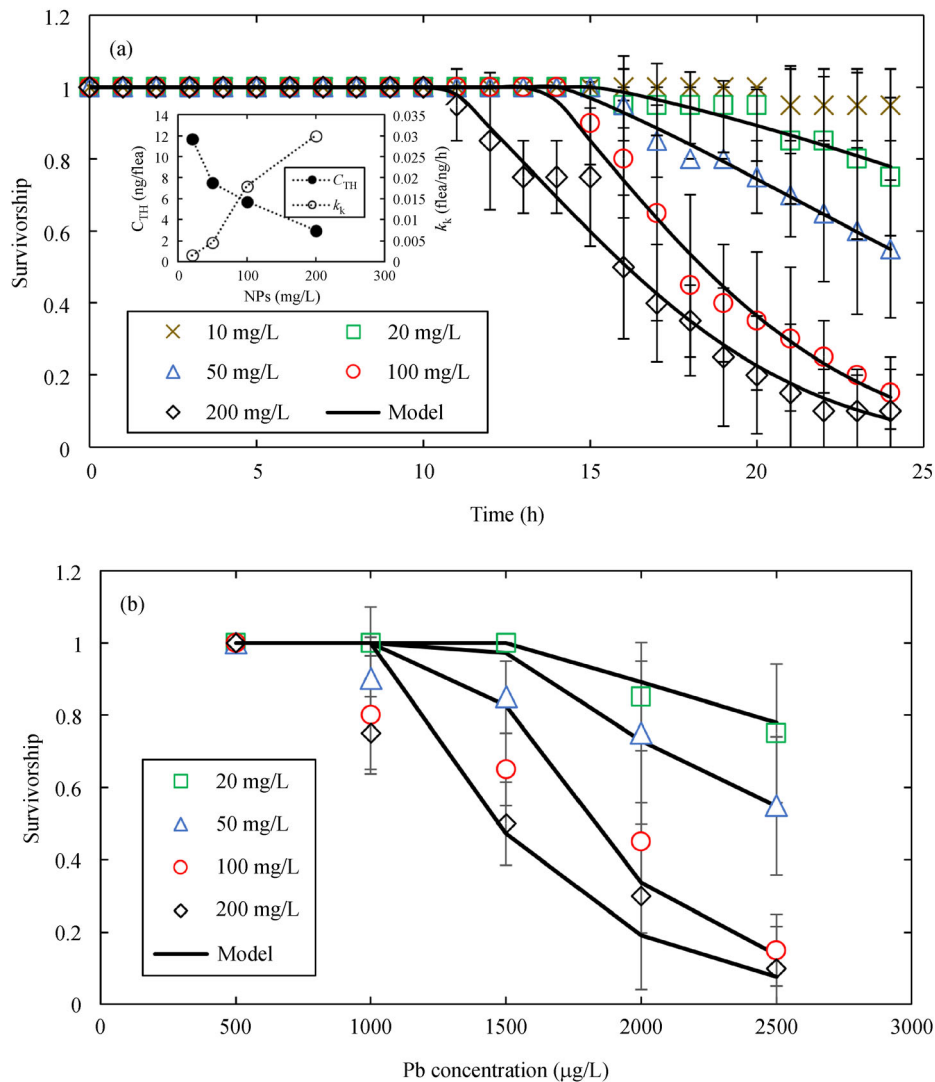

Fig. 2 Survivorship of *C. dubia* in the presence of Pb and nano-TiO$_2$. (a) The survivorship during the 24-h exposure period in test solutions that contained 2500 μg/L of Pb and various concentrations of nano-TiO$_2$ (10–200 mg/L), (b) Comparison of observed and predicted 24-h survivorship for different concentrations of nano-TiO$_2$ (20–200 mg/L) and Pb.

survivorship continued to decrease by increasing the nano-TiO_2 concentration.

Previous research indicated that nano-TiO_2 alone or Pb alone in the test concentration range (nano-TiO_2 up to 1200 mg/L; Pb up to 2500 µg/L) does not have significant toxicity on *C. dubia* (Hu et al., 2012a; Liu et al., 2019). The high toxicity from a mixture of nano-TiO_2 and Pb should be the result of a synergistic effect. The TD model, Eq. (4), was used to quantify the toxicity process based on Pb tissue accumulation. The parameters in Table 2 were substituted into Eq. (3) to calculate the Pb tissue accumulation under different nano-TiO_2 concentrations, as shown by the dotted lines in Figs. 1(a) and S1–S4. The TD modeling results, which are shown as solid curves in Fig. 2(a), are well consistent with the experimental data (all $R^2 > 0.94$). At a nano-TiO_2 concentration of 10 mg/L, the change in survivorship was negligible, as compared to the negative control group. Therefore, the data were not fitted with the TD model at this concentration. Table 3 shows the TD model parameters. The small inset in Fig. 2(a) shows the change of TD parameters as a function of nano-TiO_2 concentration. Results indicated that, with increasing nano-TiO_2 concentration, the Pb threshold (C_{TH}) in *C. dubia* was reduced, but the killing rate (k_k) was increased. For instance, the C_{TH} decreased by approximately 75% while the k_k increased 20 times, when the nano-TiO_2 concentration increased from 20 to 200 mg/L. The C_{TH} reflected the tolerance level of toxic elements, and k_k indicated the response of *C. dubia* when the toxin exceeds C_{TH} (Tan and Wang, 2012). Therefore, with a higher nano-TiO_2 concentration, the tolerance level of Pb in *C. dubia* was reduced, making Pb more toxic. In addition, the increase in k_k suggested that nano-TiO_2 makes *C. dubia* more vulnerable to the Pb attack. Our previous study showed that nano-TiO_2 alone would not lead to the death of *C. dubia* in the concentration range tested (Hu et al., 2012a). However, Pb could form a surface complex, Ti-O-Pb$^+$, with the hydroxyl group in nano-TiO_2, which may enhance the toxicity (Vohra and Davis, 1997). On one hand, the positively charged complex may interact with negatively charged biological membrane (Huang et al., 2010b). On

the other hand, the metal complex itself may play a more important role in toxicity (Sparks, 2005), as it could alter the toxicity of the metal ions or NPs (Egorova and Ananikov, 2017). Zhou et al. (2015) also reported that surface modified NPs, regardless of their type, exhibited a much higher toxicity than pristine NPs. A higher nano-TiO_2 concentration could also increase the physical body burden of *C. dubia* (Huang et al., 2010a), resulting in less tolerance to other toxic elements. These effects could reduce the C_{TH} and/or increase the k_k of test organisms. As a result, nano-TiO_2 not only served as a carrier to enhance Pb accumulation, but also participated in the toxicity process and synergistically enhanced Pb toxicity, with this effect being more evident with high nano-TiO_2 concentrations.

Based on the C_{TH} and k_k values in Table 3, we can predict the 24-h survivorship of *C. dubia* under other Pb concentration conditions, for each of the nano-TiO_2 concentrations, 20, 50, 100, and 200 mg/L, respectively. The predicted survivorship is shown as curves in Fig. 2(b). In these predictions, we first used Eq. (3) and relevant constants in Table 2 to determine Pb accumulation in the tissue. We then used Eq. (4) and constants in Table 3 to calculate corresponding survivorship. We also conducted independent experiments to validate this model prediction, shown as symbols in Fig. 2(b). The predicted survivorship was in agreement with the measured results, suggesting that the TD model parameters could accurately describe the toxicity process. The agreement between the experimental data and model prediction also suggested that nano-TiO_2 not only increases toxic element accumulation, but also participates in the toxicity process to enhance the overall toxicity. Therefore, nano-TiO_2 synergistically enhances Pb toxicity.

3.4 Effect of algae on Pb-nano-TiO_2 toxicity – experiment data and model prediction

Figure 3(a) shows the effect of algae on Pb + nano-TiO_2 toxicity. The trend of survivorship was the same as that without algae: a reduced survivorship of *C. dubia* was

Table 3 Toxicodynamic model parameters (threshold concentration C_{TH}, killing rate k_k)

Test Solution *	Predicted $C_{tissue}(24)$ (ng/flea)	C_{TH} (ng/flea)	k_k (flea/ng/h)	R^2
10 mg/L TiO_2**	9.13	N.A.	N.A.	N.A.
20 mg/L TiO_2	16.71	11.69	1.5×10^{-3}	0.94
50 mg/L TiO_2	13.07	7.53	4.6×10^{-3}	0.99
100 mg/L TiO_2	10.27	5.70	0.018	0.99
200 mg/L TiO_2	5.14	2.96	0.030	0.99
50 mg/L TiO_2 + algae***	9.73	7.53	0.002	0.95
100 mg/L TiO_2 + algae***	7.97	5.70	0.011	0.97
200 mg/L TiO_2 + algae***	4.17	2.96	0.021	0.97

Notes: * All test solutions contain 2500 µg/L of Pb. ** For 10 mg/L TiO_2, the changing in survivorship is negligible compared with negative control which is not fitted by the TD model. ***algae concentration = 1.8×10^5 cells/mL.
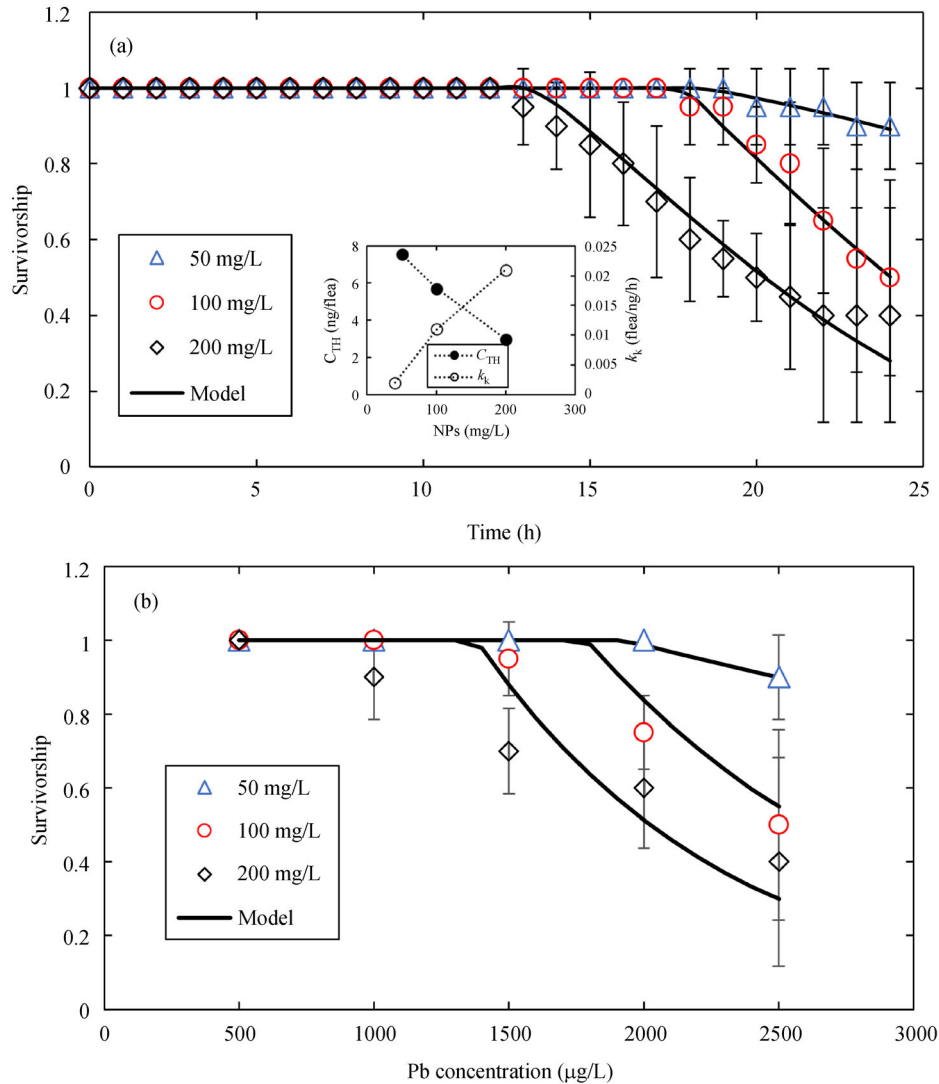
Fig. 3 Survivorship of *C. dubia* in the presence of Pb, nano-TiO$_2$, and algae. (a) The survivorship during the 24-h exposure period in test solutions that contained 2500 µg/L of Pb, various concentrations of nano-TiO$_2$ (50–200 mg/L), and 1.8 × 10^5 cells/mL of algae, (b) Comparison of observed and predicted 24-h survivorship for different concentrations of nano-TiO$_2$ (50–200 mg/L) and Pb, and 1.8 × 10^5 cells/mL of algae.

observed with increasing nano-TiO$_2$ concentrations. Compared with Fig. 2(a), algae (1.8 × 10^5 cells/mL) increased the survivorship of *C. dubia* by 0.35, 0.35, and 0.30 for 50, 100, and 200 mg/L of nano-TiO$_2$, respectively. To quantify the effect of algae on this binary toxicity, we first used Eq. (3) and associated constants in Table 2 (with 1.8 × 10^5 cells/mL of algae) to determine Pb tissue accumulation, and then used Eq. (4) to fit the time-dependent survivorship data. The model fitting results are shown as a solid line in Fig. 3(a), and the C_{TH} and k_k values for each nano-TiO$_2$ concentration are listed in Table 3. The presence of algae did not change the C_{TH} of Pb, but reduced k_k by approximately 43%, 61%, and 70% for 50, 100, and 200 mg/L of nano-TiO$_2$, respectively. These values suggest that algae reduced the *C. dubia* response – algae made

C. dubia stronger and more resistant to Pb attack. Note that the production of ROS is the primary toxicity mechanism of heavy metals (Ercal et al., 2001), and the production of antioxidants (e.g., superoxide dismutase (SOD) and glutathione (GSH)) that neutralize ROS is energy-related (Poljsak et al., 2013). As a diet, algae are an essential food source for *C. dubia* that also boost the production of antioxidants. Other than the metabolic process, it was found that some algae could directly serve as antioxidants when ingested by aquatic organisms (Romay et al., 1998). Therefore, some of the ROS produced by Pb was neutralized by the consumption of algae, reducing the killing rate of Pb. Although algae slightly reduced the accumulation of Pb (Fig. 1), the C_{TH} did not change. By considering the parameters from the TK model and the TD

model, it can be concluded that algae can occupy some of the gut space and reduce Pb uptake. They can also reduce Pb transfer to tissue where the toxicity effect occurs. Moreover, algae can mitigate the toxicity of Pb, probably through the elevation of antioxidant levels in *C. dubia*.

We also conducted independent 24-h toxicity tests to validate these TD parameters with algae. In test solutions, the concentration of Pb and nano-TiO$_2$ varied while that of algae was kept the same (1.8×10^5 cells/mL). Figure 3(b) shows the observed and predicted 24-h survivorship results, which agree with each other. This agreement suggests that this two-compartment modeling approach is also applicable to a more complicated situation: predicting the effect of nano-TiO$_2$ on heavy metal toxicity, with the presence of algae.

4   Conclusions

We found that increasing nano-TiO$_2$ concentration generally reduces Pb accumulation but increases Pb toxicity on *C. dubia*. We used a two-compartment modeling approach to quantify the toxic effect of Pb under different concentrations of nano-TiO$_2$, with or without algae. Modeling results suggested that nano-TiO$_2$ participates in the Pb toxicity process, as increasing nano-TiO$_2$ concentration reduces the Pb threshold concentration and increases the killing rate of *C. dubia*. Therefore, nano-TiO$_2$ not only serves as a carrier that changes Pb accumulation, but also synergistically enhances Pb toxicity. Algae mitigates the Pb toxicity by reducing the killing rate, without impacting the Pb threshold concentration. Importantly, this two-compartment modeling method presents a practical implement for predicting the accumulation of toxic metals in each part of *C. dubia* in the presence of NPs, and for revealing the role of NPs in toxicity.

References

Allen N S, Edge M, Verran J, Stratton J, Maltby J, Bygott C (2008). Photocatalytic titania based surfaces: Environmental benefits. Polymer Degradation & Stability, 93(9): 1632–1646

Bundschuh M, Filser J, Lüderwald S, McKee M S, Metreveli G, Schaumann G E, Schulz R, Wagner S (2018). Nanoparticles in the environment: Where do we come from, Where do we go to? Environmental Sciences Europe, 30(1): 6

Cai L, Sun X, Hao D, Li S, Gong X, Ding H, Yu K (2020). Sugarcane bagasse amendment improves the quality of green waste vermicompost and the growth of Eisenia fetida. Frontiers of Environmental Science & Engineering, 14(4): 61

Cedergreen N, Dalhoff K, Li D, Gottardi M, Kretschmann A C (2017). Can toxicokinetic and toxicodynamic modeling be used to understand and predict synergistic interactions between chemicals? Environmental Science & Technology, 51(24): 14379–14389

Dudefoi W, Moniz K, Allen-Vercoe E, Ropers M H, Walker V K (2017). Impact of food grade and nano-TiO$_2$ particles on a human intestinal community. Food and Chemical Toxicology, 106(Pt A): 242–249

Ebert D P (2005).Ecology, Epidemiology, and Evolution of Parasitism in *Daphnia*. Bethesda (MD): National Library of Medicine (USA), National Center for Biotechnology Information

Egorova K S, Ananikov V P (2017). Toxicity of metal compounds: Knowledge and myths. Organometallics, 36(21): 4071–4090

EPA (1994). Using toxicity tests in ecological risk assessment. Washington, DC: Environmental Protection Agency

EPA (2002). Methods for measuring the acute toxicity of effluents and receiving waters to freshwater and marine organisms. Washington, DC: Environmental Protection Agency

Ercal N, Gurer-Orhan H, Aykin-Burns N (2001). Toxic metals and oxidative stress part I: Mechanisms involved in metal-induced oxidative damage. Current Topics in Medicinal Chemistry, 1(6): 529–539

Fan W, Cui M, Liu H, Wang C, Shi Z, Tan C, Yang X (2011). Nano-TiO$_2$ enhances the toxicity of copper in natural water to *Daphnia magna.* Environmental Pollution (Barking, Essex: 1987), 159(3): 729–734

Gillis P L, Chow-Fraser P, Ranville J F, Ross P E, Wood C M (2005). Daphnia need to be gut-cleared too: the effect of exposure to and ingestion of metal-contaminated sediment on the gut-clearance patterns of *D. magna.* Aquatic Toxicology (Amsterdam, Netherlands), 71(2): 143–154

Horton P A, Rowan M, Webster K E, Peters R H (1979). Browsing and grazing by cladoceran filter feeders. Canadian Journal of Zoology, 57(1): 206–212

Hu J, Shipley H J (2012). Evaluation of desorption of Pb (II), Cu (II) and Zn (II) from titanium dioxide nanoparticles. Science of the Total Environment, 431: 209–220

Hu J, Wang D, Forthaus B E, Wang J (2012b). Quantifying the effect of nanoparticles on As(V) ecotoxicity exemplified by nano-Fe$_2$O$_3$ (magnetic) and nano-Al$_2$O$_3$. Environmental Toxicology and Chemistry, 31(12): 2870–2876

Hu J, Wang D, Wang J, Wang J (2012a). Toxicity of lead on *Ceriodaphnia dubia* in the presence of nano-CeO$_2$ and nano-TiO$_2$. Chemosphere, 89(5): 536–541

Huang C P, Chou H W, Tseng Y H, Fan M (2010a). Responses of *Ceriodaphnia dubia* to photocatalytic nano-titanium dioxide particles. In: Fan M, Huang C, Bland A, Wang Z, Slimane R, Wright I, eds. Environanotechnology. Amsterdam: Elsevier, 1–21

Huang Y W, Wu C H, Aronstam R S (2010b). Toxicity of transition metal oxide nanoparticles: Recent insights from in vitro studies. Materials (Basel), 3(10): 4842–4859

ICMM (2007). Health Risk Assessment Guidance for Metals. Fact Sheet

4. London: International Council on Mining and Metals

Kerper L E, Hinkle P M (1997). Cellular uptake of lead is activated by depletion of intracellular calcium stores. Journal of Biological Chemistry, 272(13): 8346–8352

Kiela P R, Ghishan F K (2016). Physiology of intestinal absorption and secretion. Best Practice & Research. Clinical Gastroenterology, 30(2): 145–159

Lademann J, Weigmann H, Rickmeyer C, Barthelmes H, Schaefer H, Mueller G, Sterry W (1999). Penetration of titanium dioxide microparticles in a sunscreen formulation into the horny layer and the follicular orifice. Skin Pharmacology and Applied Skin Physiology, 12(5): 247–256

Li F, Liang Z, Zheng X, Zhao W, Wu M, Wang Z (2015). Toxicity of nano-TiO$_2$ on algae and the site of reactive oxygen species production. Aquatic Toxicology (Amsterdam, Netherlands), 158: 1–13

Liu X, Wang J (2020). Algae (*Raphidocelis subcapitata*) mitigate combined toxicity of microplastic and lead on Ceriodaphnia dubia. Frontiers of Environmental Science & Engineering, 14(6): 97

Liu X, Wang J, Huang Y W (2021). Quantifying the effect of nano-TiO$_2$ on the toxicity of lead on *C. dubia* using a two-compartment modeling approach. Chemosphere, 263: 127958

Liu X, Wang J, Huang Y W, Kong T (2019). Algae (*Raphidocelis*) reduce combined toxicity of nano-TiO$_2$ and lead on *C. dubia*. Science of the Total Environment, 686: 246–253

López-Serrano A, Olivas R M, Landaluze J S, Cámara C (2014). Nanoparticles: A global vision. Characterization, separation, and quantification methods. Potential environmental and health impact. Analytical Methods, 6(1): 38–56

O'Regan B, Grätzel M (1991). A low-cost, high-efficiency solar cell based on dye-sensitized colloidal TiO$_2$ films. Nature, 353(6346): 737–740

Poljsak B, Šuput D, Milisav I (2013). Achieving the balance between ROS and antioxidants: when to use the synthetic antioxidants. Oxidative Medicine and Cellular Longevity, 2013: 956792

Roell K R, Reif D M, Motsinger-Reif A A (2017). An introduction to terminology and methodology of chemical synergy—Perspectives from across disciplines. Frontiers in Pharmacology, 8: 158

Romay C, Armesto J, Remirez D, González R, Ledon N, García I (1998). Antioxidant and anti-inflammatory properties of C-phycocyanin from blue-green algae. Inflammation Research, 47(1): 36–41

Roy D, Greenlaw P N, Shane B S (1993). Adsorption of heavy metals by green algae and ground rice hulls. Journal of Environmental Science and Health, Part A: Environmental Science and Engineering, 28(1): 37–50

Sparks D L (2005). Toxic metals in the environment: the role of surfaces. Elements, 1(4): 193–197

Tan C, Fan W H, Wang W X (2012). Role of titanium dioxide nanoparticles in the elevated uptake and retention of cadmium and zinc in *Daphnia magna*. Environmental Science & Technology, 46(1): 469–476

Tan C, Wang W X (2017). Influences of TiO$_2$ nanoparticles on dietary metal uptake in *Daphnia magna*. Environmental Pollution (Barking, Essex : 1987), 231(Pt 1): 311–318

Tan L Y, Huang B, Xu S, Wei Z B, Yang L Y, Miao A J (2017). Aggregation reverses the carrier effects of TiO$_2$ nanoparticles on cadmium accumulation in the waterflea *Daphnia magna*. Environmental Science & Technology, 51(2): 932–939

Tan Q G, Wang W X (2012). Two-compartment toxicokinetic-toxicodynamic model to predict metal toxicity in *Daphnia magna*. Environmental Science & Technology, 46(17): 9709–9715

Vohra M S, Davis A P (1997). Adsorption of Pb(II), NTA, and Pb(II)-NTA onto TiO$_2$. Journal of Colloid and Interface Science, 194(1): 59–67

Wang D, Hu J, Forthaus B E, Wang J (2011b). Synergistic toxic effect of nano-Al$_2$O$_3$ and As(V) on *Ceriodaphnia dubia*. Environmental Pollution (Barking, Essex: 1987), 159(10): 3003–3008

Wang D, Hu J, Irons D R, Wang J (2011a). Synergistic toxic effect of nano-TiO and As(V) on *Ceriodaphnia dubia*. Science of the Total Environment, 409(7): 1351–1356

Wani A L, Ara A, Usmani J A (2015). Lead toxicity: A review. Interdisciplinary Toxicology, 8(2): 55–64

Zhou Z, Son J, Harper B, Zhou Z, Harper S (2015). Influence of surface chemical properties on the toxicity of engineered zinc oxide nanoparticles to embryonic zebrafish. Beilstein Journal of Nanotechnology, 6: 1568–1579